Published OnlineFirst April 27, 2010; DOI: 10.1158/1535-7163.MCT-09-1163

Research Article

Molecular Cancer Therapeutics

Transcriptional Analysis of an E2F Gene Signature as a Biomarker of Activity of the Cyclin-Dependent Kinase Inhibitor PHA-793887 in Tumor and Skin Biopsies from a Phase I Clinical Study

Giuseppe Locatelli[1], Roberta Bosotti[1], Marina Ciomei[1], Maria G. Brasca[1], Raffaele Calogero[2], Ciro Mercurio[3], Francesco Fiorentini[4], Matteo Bertolotti[1], Emanuela Scacheri[1], Angela Scaburri[1], Arturo Galvani[1], Enrico Pesenti[1], Thierry De Baere[5], Jean-Charles Soria[5], Vladimir Lazar[5], and Antonella Isacchi[1]

Abstract

A transcriptional signature of the pan–cyclin-dependent kinase (Cdk) inhibitor PHA-793887 was evaluated as a potential pharmacodynamic and/or response biomarker in tumor and skin biopsies from patients treated in a phase I clinical study. We first analyzed the expression of a number of known E2F-dependent genes that were predicted to be modulated after Cdk2 and Cdk4 inhibition in xenograft tumor and skin samples of mice treated with the compound. This panel of 58 selected genes was then analyzed in biopsies from seven patients treated with PHA-793887 in a phase I dose escalation clinical trial in solid tumors. Quantitative real-time PCR or microarray analyses were done in paired skin and tumor biopsies obtained at baseline and at cycle 1. Analysis by quantitative real-time PCR of the signature in skin biopsies of patients treated at three different doses showed significant transcriptional downregulation with a dose-response correlation. These data show that PHA-793887 modulates genes involved in cell cycle regulation and proliferation in a clinical setting. The observed changes are consistent with its mechanism of action and correlate with target modulation in skin and with clinical benefit in tumors. *Mol Cancer Ther; 9(5); 1265–73. ©2010 AACR.*

Introduction

Gene expression analysis of tumor biopsies has been successfully applied to provide improved classification of tumor types and subpopulations and to the identification of prognostic and predictive biomarkers that will significantly contribute to patient stratification and possibly lead to identification of new pharmacologic targets (1, 2). On the other hand, an early development biomarker analysis that attempts to replicate preclinical pharmacokinetic/pharmacodynamic models requires pretreatment and posttreatment samples, limiting the analysis to patients for which tumor biopsies can be obtained. For this reason, other biological samples, such as blood, skin, and hair follicles, are being studied as surrogate tissues for biomarker analysis (3–5).

The analysis of transcriptional modulation can be particularly useful to follow the effects of drugs that have a direct influence on gene expression, such as inhibitors of the cyclin-dependent kinases (Cdk), a family of key regulators of cell cycle progression and transcription. In particular, Cdk2 and Cdk4 are responsible for phosphorylation of the retinoblastoma (Rb) protein, causing the release and activation of the E2F transcription factors, leading to G_1-S transition and the initiation of DNA replication (6–8). The importance of the Rb-E2F pathway in the regulation of cell proliferation is illustrated by the observation that this pathway is very frequently disrupted in tumors as a consequence of different molecular defects (reviewed in refs. 9, 10). The combined use of promoter occupancy arrays and gene expression profiling has resulted in the broad identification of genes that are transcriptionally dependent on the activator members of the E2F family, including genes that control cell cycle progression and DNA replication (11–16).

A phase I clinical trial of the pan-Cdk inhibitor PHA-793887 was recently completed. In preclinical studies, *in vitro* and *in vivo* treatment of the A2780 ovarian carcinoma tumor cell line with PHA-793887 resulted as expected in inhibition of Rb phosphorylation due to Cdk2 and Cdk4 inhibition, which could be followed by

Authors' Affiliations: [1]Business Unit Oncology, Nerviano Medical Sciences S.r.l., Nerviano (MI), Italy; [2]Bioinformatics and Genomics Unit, Dipartimento di Scienze Cliniche e Biologiche, Università di Torino, Orbassano (TO), Italy; [3]Genextra Group, Milano, Italy; [4]Drug Metabolism, Pharmacokinetics and Attrition-Reducing Technologies, Accelera, Nerviano, Italy; and [5]Institut Gustave Roussy, Villejuif Cedex, France

Note: Supplementary material for this article is available at Molecular Cancer Therapeutics Online (http://mct.aacrjournals.org/).

G. Locatelli and R. Bosotti contributed equally to this work.

Corresponding Author: Antonella Isacchi, Nerviano Medical Sciences srl, Viale Pasteur, 10, Casella postale N.11, 20014 Nerviano (MI), Italy. Phone: 39-331581285; Fax: 39-331581267. E-mail: antonella.isacchi@nervianoms.com

doi: 10.1158/1535-7163.MCT-09-1163

©2010 American Association for Cancer Research.

Downloaded from mct.aacrjournals.org on September 19, 2021. © 2010 American Association for Cancer Research.

Published OnlineFirst April 27, 2010; DOI: 10.1158/1535-7163.MCT-09-1163

Western blot or immunohistochemical analyses using anti–phospho-Rb antibodies (17).

Because a decrease in Rb phosphorylation is expected to affect transcription of E2F-dependent genes, the effects of the drug on the target genes expression were also analyzed by quantitative real-time PCR (qRT-PCR) analysis in A2780 *in vitro* and in xenograft mice, as well as in mouse skin samples, to monitor transcriptional regulation following compound treatment.

Here, we report the identification of a 58-gene signature enriched in E2F-dependent genes that we believe could be used as pharmacodynamic biomarker of PHA-793887 activity in clinical studies, and describe the observed modulation of this signature in paired skin and tumor biopsies of patients treated with PHA-793887 in a phase I clinical trial.

Materials and Methods

Cell culture and treatments. A2780 (human adenocarcinoma ovary) and MCF7 (human mammary adenocarcinoma) cells (25,000/cm^2) from the European Collection of Animal Cell Cultures were seeded in T-75 tissue culture flasks (Corning) in RPMI 1640 (pH 7.4; Life Technologies) supplemented with 10% fetal bovine serum (EuroClone Australia, U.S. Department of Agriculture approved, lot. EUS003383), 2 mmol/L L-glutamine (Life Technologies), and 1× penicillin-streptomycin (Life Technologies). After 24 hours, cells were treated with 1 μmol/L PHA-793887 (A2780) or 6 μmol/L PHA-793887 (MCF7) for 6 hours and harvested by lysis in Buffer RLT (Qiagen).

In vivo *treatments and pharmacokinetic analysis.* All animal experimental procedures complied with the Guide for the Care and Use of Laboratory Animals (Institute for Laboratory Animal Research, 1996).

A2780 human ovarian adenocarcinoma-bearing CD-1 nude mice (Charles River Breeding Laboratories) were treated with 15 or 30 mg/kg of PHA-793887 once a day by i.v. route for 2 days. Animals were sacrificed at 1.5, 6, and 24 hours after the last treatment, and tumor slices from mice treated with compound or vehicle (n = 9 animals per group) were collected and immediately soaked in RNAlater solution (Qiagen) for gene expression analysis. For pharmacokinetic analysis, plasma samples were collected from six animals at each time interval and analyzed by liquid chromatography-tandem mass spectrometry. Data were evaluated by nonlinear mixed effect modeling. Plasma levels of the compound were fitted using a two-compartment model with bolus input and first-order output mean, and random parameters were considered in the following equation: Pi = P·exp (η). The random effects were considered normal distributed with zero mean and variance ω^2.

CD-1 mice were treated with 30 mg/kg of PHA-793887 by i.v. route once a day for 2 days and sacrificed at different time points after treatment. A strip of back skin (1 × 0.2 cm) from animals sacrificed 1.5 or 6 hours after the last treatment with compound (n = 6) or vehicle (n = 6) was excised and placed in RNAlater solution for gene expression analysis. For pharmacokinetic analysis, plasma samples were collected for three animals at 5 minutes and 0.5, 1, 3, 6, and 24 hours after the last treatment, as already described. Pharmacodynamic parameters were calculated by standard noncompartmental analysis.

RNA extraction from preclinical samples. Skin or tumor biopsies (>20 mg) were collected in RNAlater solution (10 mL/mg of tissue) and incubated at least 2 hours at room temperature before storage at −20°C. Before RNA extraction, the biopsies were transferred in Eppendorf with 600 μL of Qiagen lysis buffer RLT/B-mer (1 mL:10 μL) and a stainless steel bead (5 mm) and then homogenized using mixer Retsch PBI MM300. The homogenized samples were centrifuged for 3 minutes at maximum speed, and supernatant was transferred to a fresh Eppendorf tube. Total RNA was purified using the RNeasy kit (Qiagen) following the manufacturer's instructions and quantified by spectrophotometric evaluation at 260 and 280 nm.

RNA extraction from clinical biopsies. Skin biopsies were obtained with 3-mm punch procedure, and tumor biopsies were obtained with 18-gauge Trucut procedure under radiology imaging and verified to contain ≥80% tumor cellularity. RNA extraction was done using Trizol reagent (Invitrogen) according to the manufacturer's instructions. RNA quantity and quality was assessed using NanoDrop ND-1000 UV-VIS spectrophotometer (NanoDrop p/n ND-1000) and the Agilent 2100 Bioanalyzer (42947CA).

Western blot analysis. Total protein lysates from A2780 or MCF7 cells after treatment with PHA-793887 were resolved by SDS-PAGE, transferred onto nitrocellulose membrane (Hybond ECL, GE Healthcare), and hybridized with specific antibodies anti–phospho-Rb Thr^{821} (Invitrogen), anti–phospho-Rb Ser$^{807/811}$ (Cell Signaling), anti–total Rb (BD Pharmingen), and anti–phospho-nucleophosmin (NPM) Thr^{199} (Cell Signaling).

qRT-PCR analysis. Total RNA (0.5 μg) was converted to single-stranded cDNA with the Taqman Reverse Transcription Reagents (Applied Biosystems). qRT-PCR was done with the ABI Prism 7900 Sequence Detection System (Applied Biosystems).

Gene expression levels in samples were normalized with respect to an average of four housekeeping genes (*Rrn18s*, *Actb*, *Ppia*, and *Gusb*) and relative to a calibrator sample (Stratagene human tissue panel I and IV RNA retrotranscribed mix). The expression value (E) for each gene was calculated as $E = 2^{-\Delta\Delta Ct}$, where

$$\Delta\Delta Ct = (Ct_{\text{Target Gene}} - Ct_{\text{Housekeeping}})_{\text{Sample}} - (Ct_{\text{Target Gene}} - Ct_{\text{Housekeeping}})_{\text{Calibrator}}$$

and

$$Ct_{\text{Housekeeping}} = \text{average}(Ct_{\text{Rrn18s}}, Ct_{\text{Actb}}, Ct_{\text{Ppia}}, Ct_{\text{Gusb}})$$

Downloaded from mct.aacrjournals.org on September 19, 2021. © 2010 American Association for Cancer Research.

Published OnlineFirst April 27, 2010; DOI: 10.1158/1535-7163.MCT-09-1163

Average data from treated and control groups obtained for each gene were used for hierarchical clustering of preclinical skin and tumor samples. Hierarchical clustering was done using TMEV (18). For clinical skin biopsies, data are presented as fold change after treatment.

Microarray analysis. Agilent Gene Expression Microarrays (4x44k Whole Human Genome Arrays, reference G4112F) were used.

Probe synthesis, hybridization, and scanning were done according to standard operation procedures (Reference Protocol: Agilent Technologies "Two-Color Microarray-Based Gene Expression Analysis," version 5.0.1).

Data processing was done with Bioconductor using Limma package (19). Background distribution of red and green dyes was evaluated for all arrays. Data were normalized within arrays with Lowess (20). Modulated genes were identified by comparing RNA from before versus after biopsies in dye swap.

Microarray data were submitted to the Gene Expression Omnibus database (accession number GSE18553; ref. 21).

Statistical analysis. Overall gene signature modulations in clinical tumor and skin biopsies were summarized in a metagene (i.e., the algebraic sum of positive and negative fold changes of the gene signature for each specimen). Differences in metagene values among clinical groups were evaluated by means of conventional *t* test.

Principal component regression classification was done using the PDMCLASS package implemented in Bioconductor (19). Classification specificity was assessed doing principal component regression classification on 1,000 randomly selected signatures of size comparable with the previously detected signature using oneChannelGUI package (22).

Results

Preclinical identification of a 58-gene signature modulated by PHA-793887. The ATP-competitive kinase inhibitor PHA-793887 was found to potently inhibit Cdk2 (IC_{50}, 8 nmol/L), Cdk1 (IC_{50}, 60 nmol/L), Cdk4 (IC_{50}, 62 nmol/L), Cdk9 (IC_{50}, 138 nmol/L), and glycogen synthase kinase 3β (IC_{50}, 79 nmol/L) in biochemical assays while sparing (IC_{50}, >10 μmol/L) 35 additional tyrosine and serine-threonine kinases tested (17). Treatment of A2780 tumor cell line with PHA-793887 *in vitro* was previously shown by Western blot analysis to partially inhibit Rb phosphorylation at 1 μmol/L and almost completely at 3 μmol/L (17). To identify genes modulated by Cdk2 and Cdk4 inhibition, we exploited the available literature to select a panel enriched with known E2F-dependent genes involved in cell cycle regulation and transcriptional control, DNA replication and repair, chromosome organization, mitosis, and apoptosis (Table 1; refs. 11–16). We then analyzed by qRT-PCR the expression of these genes in the A2780 tumor cell line treated with 1 μmol/L PHA-793887 *in vitro*, a concentration that was confirmed by Western blot analysis to partially inhibit phosphorylation of the Cdk2 substrates Rb and NPM (Supplementary Fig. S1). A general downregulation of the signature was observed, although with low fold changes (40 genes with fold change ≥1.5, of which 11 genes with fold change ≥2; Supplementary Fig. S2). All genes were down-modulated as expected, with the exception of *Jun B, CCND1*, and *EGR1*, a gene previously described to be upregulated also following treatment with other Cdk inhibitors (23, 24). To verify that this effect was not specific for A2780 cell line, we then analyzed the signature regulation after treatment of the mammary adenocarcinoma MCF7 cell line with 6 μmol/L PHA-793887, a concentration able to significantly inhibit Rb and NPM phosphorylation (Supplementary Fig. S1). We observed a strong modulation of the signature also in MCF7 (50 genes with fold change ≥1.5, of which 43 genes with fold change ≥2). All genes were down-modulated, with the exception of *Jun B* and *EGR*, which were again upregulated.

For *in vivo* analysis, A2780 cells were transplanted s.c. in CD-1 nude mice that were subsequently treated for 2 days with PHA-793887 at 15 or 30 mg/kg and then sacrificed 1.5, 6, and 24 hours after treatment. These doses, when administered daily for 10 days in similar

Table 1. Genes included in the 58-gene signature

Functional category	Genes
Cell cycle regulation and transcription control	*CCNA2, CCND1, CCNE2, CDC25A, CKS1B, E2F2, E2F8, EGR1, HMGA1*
DNA replication and DNA repair	*CDC6, MCM2, MCM3, MCM4, MCM5, MCM6, MCM7, MSH2, ORC1L, ORC6L, POLA, RFC3, RRM1, RRM2, RPA3, TK1, TYMS*
Chromosome organization	*CENPA, H1FX, HIST1H1C, HIST1H2AA, HIST1H2AE, HIST1H3H, HIST1H4C, H2AFZ, HIST2H2BE, HIST2H4, H3F3B*
Mitosis and mitotic spindle checkpoint	*ASPM, C13ORF3, CCNB1, CCNB2, CDC20, ESPL1, PLK1, PLK4, STK6, TP53, WEE1*
Apoptosis	*APAF1, CASP3*
Miscellaneous	*CCNF, DHFR, FLJ40629, JUNB, KIF2C, LOC146909, MKI67, RNU2*

Downloaded from mct.aacrjournals.org on September 19, 2021. © 2010 American Association for Cancer Research.

Published OnlineFirst April 27, 2010; DOI: 10.1158/1535-7163.MCT-09-1163

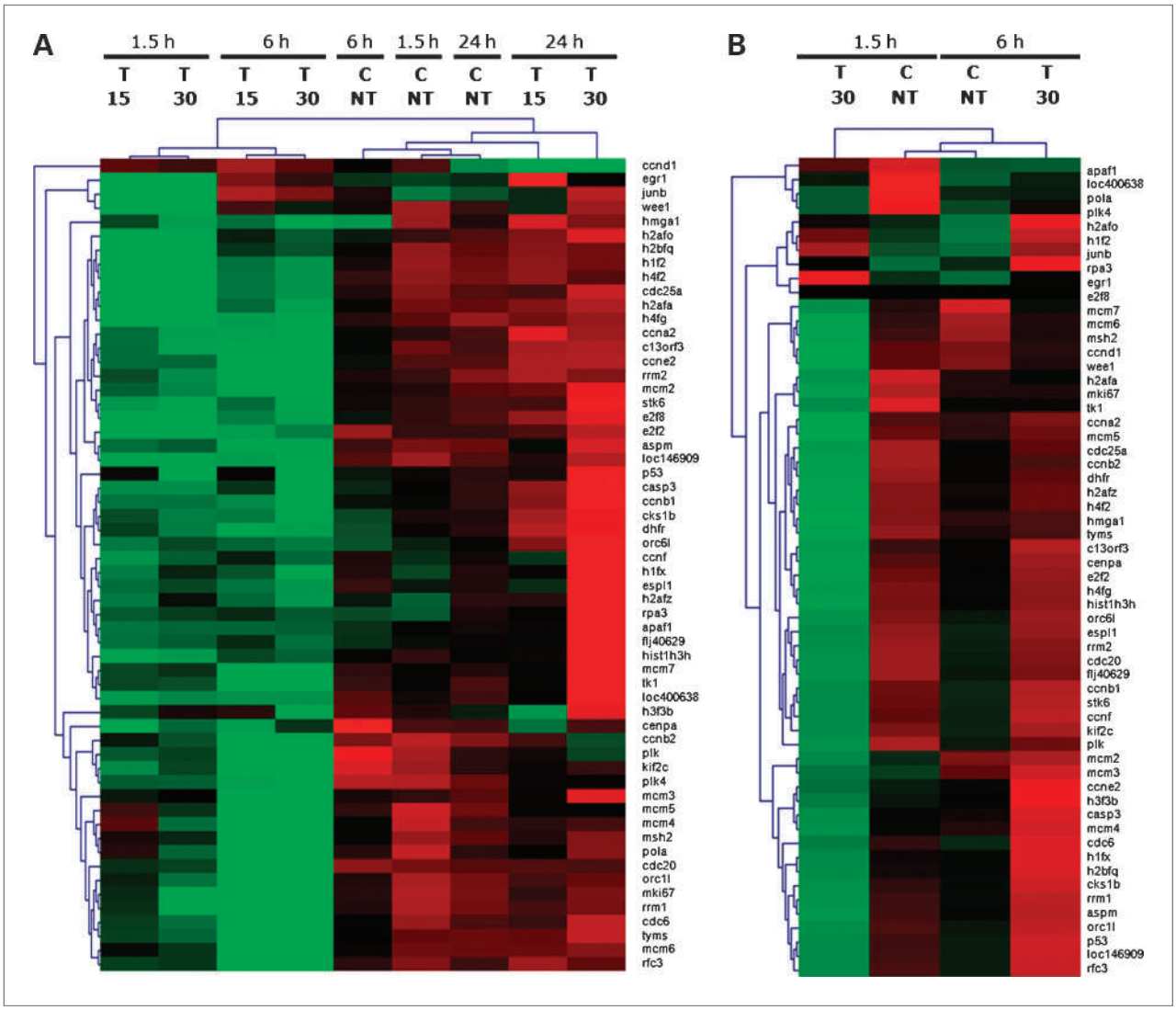

Figure 1. A, hierarchical cluster analysis of qRT-PCR data on *ex vivo* tumor samples at 1.5, 6, and 24 h after the last treatment with PHA-793887 at 15 or 30 mg/kg. B, same analysis in skin samples collected at 1.5 or 6 h after the last treatment with PHA-793887 at 30 mg/kg.

experiments, induced tumor growth inhibition in the range of 50% (15 mg/kg) to 75% (30 mg/kg) versus untreated mice, respectively. In addition, the dose of 30 mg/kg was shown by immunohistochemistry to significantly reduce Rb phosphorylation (17). Compound plasma levels were measured for both doses, showing an area under the curve (AUC) 0-∞ of 16.9 μmol/L·h at 15 mg/kg and of 34.5 μmol/L·h at 30 mg/kg. After reaching respective peak concentrations of 46.5 and 93.6 μmol/L, the levels of the compound at both doses quickly decreased to become undetectable by 24 hours (Supplementary Fig. S3). In agreement with the pharmacokinetic profile of the compound, a significant downregulation of the signature was observed by qRT-PCR at 1.5- and 6-hour time points (~40 genes with fold change ≥1.5 at 15 mg/kg, ~45 genes with fold change ≥1.5 at 30 mg/kg, ~50% of which with fold change ≥2 in all cases). No significant reduction of gene expression was observed at 24 hours with both doses but rather a slight trend to upregulation, which could be interpreted as a rebound effect after the downregulation observed at the earlier time points (Supplementary Fig. S2). The *EGR1* gene showed a trend to upregulation at both doses, whereas *Jun B* and *CCND1* were less consistently modulated.

Because we planned to use skin biopsies as surrogate tissue in the clinical biomarker analysis, we analyzed expression of the murine orthologues of these genes in treated mice skin. Due to the difficulty of analyzing skin biopsies in nude mice, we treated CD-1 mice for 2 days with PHA-793887 at 30 mg/kg i.v. and skin biopsies were collected at 1.5- and 6-hour time points after the last treatment. The compound plasma concentration and

Downloaded from mct.aacrjournals.org on September 19, 2021. © 2010 American Association for Cancer Research.

Published OnlineFirst April 27, 2010; DOI: 10.1158/1535-7163.MCT-09-1163

kinetics were comparable with those measured in CD-1 mice (AUC 0-∞ = 29 μmol/L·h; Supplementary Fig. S4). Significant downregulation of the 58-gene panel was also observed in skin, although with a more transient effect than in tumors, because at 1.5 hours there was a modulation at least comparable with that observed in tumors at the early time points (48 genes with fold change ≥1.5, ~75% of which with fold change ≥2), but already at 6 hours there was a trend to upregulation due to the putative rebound effect, as observed in tumors (Supplementary Fig. S2). Overall, despite variations in the expression levels of individual genes, there was a consistent trend to downregulation of the signature after PHA-793887 treatment *in vitro* and *in vivo*, both in tumor and in skin. The *EGR1* gene showed a trend to upregulation, whereas *Apaf1, cyclin D1, Jun B*, and *p53* showed little or no modulation in all conditions tested. Hierarchical clustering of the *in vivo* qRT-PCR data for this panel of genes allowed separation of treated from control tumor samples both at 1.5 and 6 hours, whereas at 24 hours the overall gene signature was more similar to controls, as already noted (Fig. 1A). A good separation was also obtained in skin at 1.5 hours, whereas treated samples at 6 hours were clustered with controls, as expected due to the transient signature modulation observed, which could be due to several reasons, including, for example, a diverse proliferative index of this tissue or a different drug distribution or metabolism in the CD-1 mice (Fig. 1B).

Gene signature analysis in clinical biopsies. The clinical study CDKC-887-001 was a phase I trial open-label, nonrandomized, dose-escalation study in patients with advanced metastatic solid tumors (25). A synopsis of the tumor samples and of the corresponding pharmacodynamic and clinical parameters relevant for this biomarker study is reported in Table 2. Patients were to receive multiple cycles of PHA-793887, administered as 1-hour i.v. infusion on days 1, 8, and 15 in a 28-day cycle, with treatment continuation until disease progression. A total of 19 patients were treated at four dose levels: 11 mg/m^2 (n = 4), 22 mg/m^2 (n = 3), 44 mg/m^2 (n = 9), and 66 mg/m^2 (n = 3). The 44 mg/m^2 dose cohort was expanded to nine patients to further evaluate safety, tolerability, pharmacokinetics, and biological activity. A good proportionality was observed between the administered doses and the plasma exposures (Table 2).

Transcriptional analysis, including qRT-PCR, on the 58-gene signature in skin biopsies, as well as complete microarray analysis of tumor biopsies from the same patients, was a secondary end point in the clinical protocol. For 7 of 19 patients treated at three different doses in this study, skin and tumor biopsies were collected in parallel at baseline before treatment and during the second administration in cycle 1 within 2 to 6 hours from the end of the day 8 infusion. This timing was chosen based on the kinetics observed for gene modulation during preclinical studies. To correlate gene expression analysis with clinical outcome, for the scope of this study, patients were divided in two groups: patients 3, 6, 8, and 15 who completed ≥4 cycles of treatment (i.e., ≥4 mo on study) and patients 2, 9, and 16 who completed <4 cycles (i.e., <4 mo on study). Patients included in this analysis belonged to three dose cohorts: 11, 22, and 44 mg/m^2. At all three doses, there were patients who completed ≥4 cycles.

We evaluated the modulation of the 58-gene signature in skin by qRT-PCR and compared it to the changes observed for these genes by microarray analysis of the corresponding tumor samples.

As shown in Fig. 2A, a clear dose-response trend in the signature modulation was observed in skin biopsies, where a limited number of genes were already modulated in samples from patients 2, 3, and 6 treated at the lowest doses, but this number increased substantially in biopsies from patients 8, 9, 15, and 16 who had received the highest dose of 44 mg/m^2, suggesting that the signature represents a bona fide pharmacodynamic biomarker of target modulation in skin. The overall gene signature

Table 2. Synopsis of biopsies and clinical parameters for the patients included in this biomarker study

Patient no.	Site of primary tumor	Site of biopsy	PHA-793887 dose (mg/m^2)	Exposure AUC 0-∞ on day 15 (μmol/L·h)	C_{max} (μmol/L)	No. cycles received
2	Uterus leiomyosarcoma	Lung	11	1.69	0.95	2
3	**Epithelioid angiomyolipoma**	**Pelvis**	**11**	**1.64**	**0.75**	**5**
6	**Parotid gland adenocarcinoma**	**Lung**	**22**	**3.57**	**2.34**	**4**
8	**Kidney papillary carcinoma**	**Lymph node under clavicula**	**44**	**6.04**	**4.36**	**8**
9	Cholangiocarcinoma	Liver	44	6.88	4.36	3
15	**Abdominal sarcoma**	**Abdominal mass**	**44**	**5.45**	**3.69**	**4**
16	Breast carcinoma	Peritoneal	44	8.1	4.25	1

NOTE: In bold text are patients belonging to the group that completed ≥4 cycles of treatment.

Downloaded from mct.aacrjournals.org on September 19, 2021. © 2010 American Association for Cancer Research.

Published OnlineFirst April 27, 2010; DOI: 10.1158/1535-7163.MCT-09-1163

A

Patient #	2	3	6	8	9	15	16
AUC 0 - ∞ (μmol/L·h)	1,69	1,64	3,57	6,04	6,88	5,45	8,1
C_{max} (μmol/L)	0,95	0,75	2,34	4,36	4,36	3,69	4,25
Cycles in treatment	< 4 cycles	≥ 4 cycles	≥ 4 cycles	≥ 4 cycles	< 4 cycles	≥ 4 cycles	< 4 cycles
Dose (mg/m²)	11		22	44			
anaf1	-1.7	-1.1	-1.1	-1.0	-1.9	-1.8	-2.4
aspm	1.6	-1.2	-1.5	-1.4	-4.3	-3.8	-2.1
casp3	-1.2	-1.2	-1.2	-1.2	-2.4	1.1	-1.4
ccna2	-1.3	-1.2	-1.3	-2.1	-3.4	-1.3	1.0
ccnb1	-1.1	-1.7	-1.2	-1.8	-5.8	-2.3	-2.5
ccnb2	-1.4	-1.5	-1.2	-2.3	-4.8	-2.0	-1.8
ccnd1	-1.3	1.1	1.1	1.2	-1.2	-1.5	-2.3
ccne2	-1.1	-1.7	1.1	-1.4	-7.0	-4.8	-1.8
ccnf	-1.6	-1.2	1.5	-1.9	-1.9	1.1	-1.7
cdc20	-1.1	-1.8	-1.8	-2.6	-6.7	-2.1	-1.5
cdc25a	-3.2	1.3	-1.7	-24.1	-35.7	-1.9	-2.9
cdc6	-1.8	1.1	-1.0	-2.6	-8.5	-2.7	-1.7
cenpa	-1.2	-2.4	-3.1	-2.2			
cks1b	-1.2	-1.1	1.0	1.2	-1.3	-1.1	1.4
dhfr	-1.1	-1.5	-1.2	1.2	-1.8	-1.8	-1.6
e2f2	-1.2	-1.2	-1.2	-1.8	-1.9	-3.9	1.1
e2f8	-1.7	-1.3	-1.1	-2.1	-3.2	-1.6	-1.6
egr1	-1.3	1.6	1.4	1.3	-1.9	-1.3	2.8
espl1	1.4	1.2	1.3	-1.7	-2.6	-1.2	1.2
h1f2	-1.1	-1.9	-1.6	-1.4	-2.2	-2.1	-1.7
h1fx	-1.3	-1.3	-1.3	-1.7	-2.1	-1.7	-3.9
h2afa	-1.1	-2.3	-1.9	-2.9	-3.5	-1.4	-2.6
h2afo	-1.1	-2.0	-1.3	-1.5	-2.0	-1.5	-1.4
h2afz	-1.0	-1.6	-1.0	1.1	-1.9	-1.6	-1.9
h2bfo	-1.3	-1.7	-1.5	-1.6	-2.0	-1.4	-1.6
h3f3b	-1.2	-1.1	-1.1	1.1	-1.3	-1.1	-1.3
h4f2	-1.0	-2.6	-1.5	-2.4	-3.6	-2.7	-3.2
h4fq	-1.1	-2.0	-1.2	-1.7	-2.1	-2.8	-2.0
hist th3h	1.2	-1.7	-1.3	-2.2	-3.8	-2.4	-1.3
hmga1	1.1	1.1	1.2	1.1	-1.4	-1.1	-1.1
junb	-1.4	-1.2	1.6	-1.3	-1.1	-1.6	-2.3
kif2c	1.6	-1.2	-1.3	-1.6	-4.5	-2.7	-2.0
mcm2	-1.0	1.1	-1.4	-1.8	-2.4	-2.0	-1.6
mcm3	-1.6	-1.2	-1.9	-1.5	-1.5	-1.5	-2.8
mcm4	-1.1	1.2	-1.2	-1.1	-1.5	-1.5	-1.3
mcm5	-1.3	-1.6	-1.6	-1.3	-1.7	-1.7	-2.3
mcm6	-1.7	-2.3	-2.3	-1.5	-2.7	-2.6	-3.1
mcm7	-1.3	-1.5	-1.4	-1.3	-2.1	-1.7	-2.2
mki67	-1.4	-1.8	-1.4	-2.0	-4.5	-3.1	-1.3
msh2	-1.9	-1.1	-1.3	1.1	-2.0	-1.4	-2.3
orc1l	1.6	-1.2	-1.2	-1.7	-2.6	-1.1	3.6
orc6l	-2.4	-2.1	-3.1	-1.1	-1.4	-1.1	2.0
p53	-1.1	1.7	1.3	-1.0	-1.4	1.0	-1.4
plk	-1.1	-2.2	1.5	-3.4	-2.5	-1.5	-1.6
plk4	-3.3	-3.5	-2.0	-2.8	-3.6	-2.5	-5.4
pola	-1.2	1.2	1.1	1.1	-1.1	-1.1	-1.2
rfc3	-1.8	-2.1	-1.6	-1.2	-2.9	-1.3	-2.0
rnu2	-1.2	1.3	1.7	-1.4	-1.7	1.0	-1.1
rpa3	-1.8	-1.3	1.7	-5.0	-4.3	1.1	1.1
rrm1	-1.2	-1.1	-1.3	1.1	-1.1	-1.3	-1.2
rrm2	1.2	-2.0	-1.1	-2.1	-6.5	-2.6	-6.8
stk6	-1.6	-1.5	-1.1	-1.8	-1.5	-1.2	-1.3
tk1	1.4	-1.3	-1.3	-1.2	-2.1	-1.2	-1.4
tyms	1.5	-1.4	-1.1	-1.4	-1.1	-1.3	1.9
wee1	-2.9	1.1	-1.4	-1.1	-2.7	-1.0	1.2
Metagene	-54.4	-55.5	-43.8	-92.7	-182.7	-86.6	-74.6

B

Patient #	2	9	16	3	6	8	15
AUC 0 - ∞ (μmol/L·h)	1,69	6,88	8,1	1,64	3,57	6,04	5,45
C_{max} (μmol/L)	0,95	4,36	4,25	0,75	2,34	4,36	3,69
Dose (mg/m²)	11	44	44	11	22	44	44
Cycles in treatment	< 4 cycles in treatment			≥ 4 cycles in treatment			
anaf1	-1.1	-1.6	-1.9	-1.0	-1.5	-2.2	-2.9
aspm	1.3	-6.3	-1.6	-5.4	-1.6	-7.2	1.5
casp3	1.2	-1.2	-1.2	1.3	-1.1	1.6	1.1
ccna2	1.1	-1.3	1.3	-2.5	-2.3	-4.2	-2.7
ccnb1	1.2	-1.9	1.2	-2.6	-1.7	-4.9	-5.5
ccnb2	1.2	-1.7	1.7	-3.2	-1.6	-3.5	-4.6
ccnd1	-1.4	-1.0	1.9	2.1	1.5	1.0	-3.6
ccne2	1.4	-1.5	-1.5	-2.6	-1.7	-1.2	-2.4
ccnf	1.7	-2.6	-1.6	-2.2	-1.1	-2.3	-1.4
cdc20	1.1	-1.3	1.0	-1.7	-2.1	-3.5	-4.4
cdc25a	3.4	-1.8	-1.6	-2.5	-1.5	-3.3	-3.0
cdc6	4.0	-1.6	1.8	-2.2	-1.5	-2.7	-4.5
cenpa	1.0	-1.3	-1.4	-3.0	-4.4	-3.2	-5.5
cks1b	2.2	1.1	2.0	-1.5	-1.2	-1.1	-1.1
dhfr	2.6	-1.8	-1.1	-1.6	2.8	-1.4	1.2
e2f2	2.1	1.3	-2.7	-3.5	-2.4	-9.9	-1.4
e2f8	1.1	-2.1	-1.3	-2.8	-1.8	-2.8	-4.0
egr1	-2.2	5.1	2.3	16.5	2.3	2.1	1.7
espl1	1.2	-1.3	-1.7	-5.4	-1.2	-4.6	1.1
h1f2	-4.1	4.3	1.2	-1.1	-1.1	-3.0	-2.6
h1fx	-1.5	-1.9	-1.7	-1.2	-1.9	-1.3	-2.8
h2afa	-1.1	-1.1	1.3	1.2	-1.2	-2.3	1.1
h2afo	-2.5	1.5	1.2	3.3	-1.0	-2.0	-2.2
h2afz	1.7	-1.9	1.5	-1.4	-1.3	-1.6	-1.7
h2bfo	-3.5	2.0	-1.1	1.1	-1.3	-2.6	-2.4
h3f3b	-1.8	-1.2	-1.3	1.5	-1.1	-1.1	-1.7
h4f2	1.5	2.4	1.2	1.5	-1.1	-1.2	-1.4
h4fq	2.2	-1.3	-1.2	-1.3	-1.9	-1.9	-2.3
hist1h3h	1.7	1.4	1.9	1.5	1.0	-2.7	-1.3
hmga1	-1.3	1.1	-1.2	3.0	1.1	-1.0	-1.4
junb	1.2	1.1	1.4	4.8	1.4	3.1	-1.0
kif2c	-1.1	-2.5	-1.1	-2.5	-1.0	-5.4	-1.1
mcm2	1.7	-1.6	2.1	-2.4	-1.3	-2.6	-2.9
mcm3	1.1	-4.5	1.1	-2.8	-1.5	-1.8	-3.4
mcm4	1.6	-1.8	2.2	-2.4	-1.3	-2.3	-2.1
mcm5	1.8	-1.1	1.0	-2.2	-1.3	-1.3	-2.0
mcm6	1.3	-2.9	1.1	-2.3	-1.5	-1.4	-3.5
mcm7	-1.1	-1.7	-1.2	-1.8	-2.5	-3.1	-1.3
mki67	1.3	-5.0	-1.6	-2.5	-3.8	-5.2	1.2
msh2	1.2	-3.4	-1.3	-1.8	-1.3	-1.5	-1.8
orc1l	2.9	1.6	1.6	-1.8	-1.4	-3.0	-3.1
orc6l	1.7	-1.6	-5.4	4.9	1.5	1.1	1.4
p53	-1.5	-1.3	-1.2	-3.3	-1.1	1.2	-1.5
plk	1.2	2.8	1.5	-1.8	-1.1	-1.6	-1.8
plk4	1.9	-1.9	1.4	-3.1	-1.8	-3.9	-2.0
pola	1.6	-1.8	1.8	-1.7	1.0	1.3	1.1
rfc3	1.7	-3.4	-1.5	-2.6	-2.3	-3.2	1.7
rnu2							
rpa3	2.2	2.1	1.2	1.0	-1.2	-2.0	-1.3
rrm1	1.8	-1.0	1.7	-1.1	1.0	-1.3	-1.7
rrm2	4.0	-1.5	1.3	-4.0	-1.7	-2.5	-5.6
stk6	-1.0	-1.9	-1.5	-2.0	-2.1	-4.1	-4.7
tk1	4.0	1.1	3.7	-3.1	1.1	-3.8	-5.3
tyms	3.3	2.2	2.2	-2.9	1.1	-1.6	-2.7
wee1	1.1	2.6	1.1	-2.0	1.1	-1.9	-2.9
Metagene	48.1	-42.7	9.3	-55.2	-51.8	-120.9	-105.6

Figure 2. Gene expression variations (fold changes) in posttreatment versus pretreatment clinical biopsies. A, qRT-PCR analysis in skin. B, microarray analysis in tumors. Highlighted in gray, downregulated genes; light gray, fold change ≤–1.3; dark gray, fold change ≤–2. Metagene values were calculated as the sum of positive and negative fold changes. AUC, C_{max}, and number of cycles in treatment are also shown for each patient.

modulation quantified as metagene values was found to be statistically different ($P < 0.05$) between patients who were treated at the low doses of 11 and 22 mg/m^2, corresponding to an AUC of <3.5 and a C_{max} of <2.5, and those who were treated at the highest dose of 44 mg/m^2 with an AUC of >5 and a C_{max} of >3.5. We did not observe a correlation with permanence in treatment in skin ($P > 0.05$).

To analyze signature modulation in tumors, RNA from tumor biopsies was hybridized to Agilent 4x44k Whole Human Genome Microarrays according to standard procedures. Overall, >2,000 genes were modulated by treatment in each patient with an absolute fold change of >2, apart from patient 6 for which only 924 modulated genes were identified. As opposed to the results obtained in the skin, the 58-gene signature modulation in tumors did not correlate with the administered doses and exposures (Fig. 2B). Instead, we observed a higher modulation of the signature in all patients who completed ≥4 cycles of treatment, including patients 8 and 15, treated at the highest dose, but also patient 3, and to some extent patient 6, who received lower doses. Patients 2, 9, and 16 who completed <4 cycles of treatment showed a lower signature modulation in terms of both number of modulated genes and absolute fold change values, irrespective of the dose received.

The overall gene signature modulation quantified as metagene values for the group that completed ≥4 cycles versus the group that did not was found to be statistically significant by mean of t test ($P < 0.05$), whereas we did not observe any correlation with dose, AUC, or C_{max}.

Using principal component regression classification based on the 58-gene signature, we obtained a good separation between the two groups of patients, with a

Downloaded from mct.aacrjournals.org on September 19, 2021. © 2010 American Association for Cancer Research.

Published OnlineFirst April 27, 2010; DOI: 10.1158/1535-7163.MCT-09-1163

classification error of 0.14. To evaluate the specificity of this finding, we did the same test on 1,000 randomly selected signatures of comparable size and found that only 0.9% of them were able to correctly separate the two groups, suggesting that the segregation observed with the 58-gene signature could reflect a biologically relevant response in tumor tissues. Additionally, the transcriptional down-modulation of the E2F signature was not due to a general gene downregulation effect because there were no major differences in the total number of regulated genes or the number of down-modulated genes (cutoff, >2-fold) in the group of patients who completed ≥4 cycles versus the one who completed <4 cycles (Supplementary Fig. S5).

Although the observation of a higher E2F signature modulation in tumors from patients who showed the longest permanence in treatment is intriguing, we recognize that our study is of an exploratory and hypothesis-generating nature and will require confirmation by additional studies.

Discussion

The focus of this study was to compare intrapatient biomarker modulation in skin and tumor. Although we were able to collect basal biopsies for a significant number of patients, for some we could not obtain the post-treatment biopsies because they went off study for early progression or experienced adverse events, preventing the administration of the second dose and/or the biopsy collection. Despite the issues related to the collection of clinical samples, this study succeeded in obtaining a complete set of paired intrapatient pretreatment and posttreatment skin and tumor biopsies for each patient for subsequent gene expression analysis. Although the small number of available samples limits the statistical significance of the analysis, this represents a significant achievement for a phase I study, allowing a comparison of target modulation in both tissues of the same patient.

In an effort to identify the best combination of Cdk activities that will lead to the greatest efficacy with minimal toxicity, several small molecules that inhibit the function of multiple Cdks with different relative potency are currently in phase I/II studies, in addition to flavopiridol, which is already in phase III clinical trials (26–34). Because many of these molecules are potent inhibitors of Cdk2 alone or in combination with Cdk4, the functional status of the Rb pathway can be used to assist in interpretation of clinical results with respect to target modulation. In this study, we explored the possibility to follow inhibition of E2F transcriptional activation as a complementary approach to monitoring phospho-Rb levels by immunohistochemistry (35–37). This analysis can be readily done by qRT-PCR, a technology that can be more easily standardized and offers the opportunity to complete the analysis of individual samples during the progression of the clinical study, contributing supportive information relative to each individual patient.

Gene expression analysis using microarrays is increasingly being used to monitor changes in mRNA expression in response to drug treatment, but in most cases, this is limited to *in vitro* treatment of tumor cell lines (38). There are nonetheless a few examples in which gene expression patterns after treatment with kinase inhibitor drugs in clinical trials have been used to monitor target modulation. About Cdk inhibitors in particular, the transcriptional effects of roscovitine treatment in tumor biopsies from patients with undifferentiated nasopharyngeal cancer were analyzed, showing downregulation of a panel of genes including those related to apoptosis, cell cycle proliferation, DNA repair, and signal transduction likely due to inhibition of Cdk2, Cdk7, and Cdk9 (37). Very recently, candidate genes to be used as biomarkers of target modulation by the Cdk1, Cdk2, and Cdk4 inhibitor R547 were selected using preclinical data derived from microarray experiments and tested in blood samples of phase I patients (24).

To select the panel of genes to be monitored as biomarker, we exploited the amount of information that has been accumulated during the last years relative to genes that are directly regulated by the E2F activators (11–16) to compile a signature composed of E2F-dependent genes, which we found to be significantly regulated by PHA-793887 treatment during the course of preclinical studies. In the case of a well-known pathway such as that of E2F, this knowledge-based approach has an advantage with respect to the unbiased identification of genes transcriptionally modulated by the compound of interest (23, 24), in that it makes use of data obtained in several experimental models and cross-validated by multiple laboratories over the course of several years, lowering the risk of selecting genes that are preferentially modulated in the experimental conditions used or by a specific compound.

To our knowledge, this is the first time that the modulation of an E2F signature by small-molecule Cdk inhibitors is monitored in clinical studies. Here, we show that, as expected, simultaneous inhibition of multiple Cdks, including Cdk2, Cdk4, and Cdk9, induces strong downregulation of genes related to cell cycle, DNA replication, DNA repair, chromosome organization, mitosis, and apoptosis. Among the downregulated genes are *cyclin E* and *cyclin A* as well as several components of the DNA replicative complex such as *MCM2-7*, *Orc1* and *Orc6* subunits, and *CDC6*, but a reduction of mitotic genes including *Plk1*, *STK6/aur A*, *cyclin B1*, *cyclin B2*, and *Wee 1* was also observed, consistent with the *in vitro* mechanism of action of PHA-793887 (17). Although we observed a consistent trend to a general downregulation of most genes in the 58-gene signature, the extent of individual gene modulation varied in individual samples, as might be expected due to the high heterogeneity of the tumor biopsies analyzed. The metagene signature modulation, quantified as the sum of single-gene variations, can be

Downloaded from mct.aacrjournals.org on September 19, 2021. © 2010 American Association for Cancer Research.

Published OnlineFirst April 27, 2010; DOI: 10.1158/1535-7163.MCT-09-1163

better used as indicator of the overall modulation of the E2F pathway. The only gene that was consistently upregulated both in preclinical and in clinical samples was EGR1, a transcription factor that was also induced by *in vitro* treatment with roscovitine (23), as well as in blood after patient treatment with R547 (24).

Thus, activation of the E2F pathway is an important and frequent biological event, previously shown to be part of a core signature of proliferation associated with tumorigenesis (39), which seems to be modulated by pharmacologic treatment with PHA-793887.

At the beginning of preclinical studies for PHA-793887 biomarker development, we explored the use of different surrogate tissues, including bone marrow, peripheral blood mononuclear cells (PBMC), and skin. Despite a good expression modulation of the gene signature in bone marrow, we excluded this tissue due to the invasive sampling procedures requested in a clinical setting. Instead, we did not find significant gene modulation in unstimulated PBMCs, and we did not explore the use of stimulated PBMCs because we were afraid that sample manipulation could introduce additional gene expression variability, resulting in skewed expression fold changes. For these reasons, we focused instead on skin, which, although containing relatively few proliferating cells, is a continuously developing system encompassing several distinct stem cell populations, where many of the most important developmental signaling networks are active (reviewed in ref. 3).

Although previous studies using skin biopsies as a surrogate tissue for biomarker analysis have been mainly focused on epidermal growth factor receptor inhibitors, we and others have shown examples showing that it is possible to monitor pharmacodynamic markers of Cdk inhibition in preclinical as well as clinical skin biopsies (40–42).

In addition, it has been reported that plucked hairs can be leveraged as a source of pharmacodynamic markers for other cell cycle inhibitors and could represent an alternative tissue for the E2F gene signature evaluation (43).

The data presented here suggest that the E2F pathway can be transcriptionally monitored in clinical biopsies after treatment with Cdk inhibitors and show that whereas its regulation correlates with drug exposure in skin, in the tumors there is no direct correlation with the dose received. Rather, signature modulation could reflect the genetic background of individual specimens and is potentially predictive of the clinical response. Different explanations can be envisioned for lack of transcriptional regulation in tumors of patients 9 and 16 who were treated at the highest doses, including a failure of the drug to reach sufficient concentrations in the tumor environment, the independence of E2F functions from Cdk activity, as can be expected for instance in those tumors where the Rb protein is lost or not functional, and, more in general, due to the complexity of the E2F pathways in cancers (reviewed in ref. 44).

The gene signature modulation observed in skin would suggest that it might be worthwhile to further explore intermediate doses between 22 mg/m^2, where a degree of target modulation can already be observed, and 44 mg/m^2, where there is full target modulation, but at which limiting toxicity occurred. Although the data presented here were obtained on a small number of cases, we nonetheless believe that they provide firm evidence for the rationale and, perhaps more importantly, for the feasibility of systematically measuring transcriptional biomarker modulation during phase I clinical testing. These data prompt additional testing of this gene signature in clinical studies with Cdk inhibitors to further validate its application as a potential pharmacodynamic and/or response biomarker.

Disclosure of Potential Conflicts of Interest

No potential conflicts of interest were disclosed.

Acknowledgments

We thank the patients and their families, the nurses, and the study investigators of Institut Gustave Roussy (Villejuif Cedex, France); Maria Adele Pacciarini for clinical study management; Rachele Alzani and Wilma Pastori for compound characterization; Valter Croci and the Experimental Therapy group for animal treatment; Laura Raddrizzani for technical support; Barbara Valsasina for useful discussions; and Giulio Draetta for critical reading of the manuscript.

The costs of publication of this article were defrayed in part by the payment of page charges. This article must therefore be hereby marked *advertisement* in accordance with 18 U.S.C. Section 1734 solely to indicate this fact.

Received 12/15/2009; revised 03/01/2010; accepted 03/18/2010; published OnlineFirst 04/27/2010.

References

1. Chung CH, Bernard PS, Perou CM. Molecular portraits and the family tree of cancer. Nat Genet 2002;32 Suppl:533–40.
2. van't Veer LJ, Bernards R. Enabling personalized cancer medicine through analysis of gene-expression patterns. Nature 2008;452:564–70.
3. Phillips RL, Sachs AB. Skin biopsies for the measurement of clinical pharmacodynamic biomarkers. Curr Opin Biotechnol 2005;16:687–90.
4. Williams R, Baker AF, Ihle NT, Winkler AR, Kirkpatrick L, Powis G. The skin and hair as surrogate tissues for measuring the target effect of inhibitors of phosphoinositide-3-kinase signaling. Cancer Chemother Pharmacol 2006;55:444–50.
5. Colburn WA. Biomarkers in drug discovery and development: from target identification through drug marketing. J Clin Pharmacol 2003;43:329–41.
6. Weinberg RA. The retinoblastoma protein and cell cycle control. Cell 1995;81:323–30.
7. Lundberg AS, Weinberg RA. Functional inactivation of the retinoblastoma protein requires sequential modification by at least two distinct cyclin-cdk complexes. Mol Cell Biol 1998;18:753–61.
8. Harbour JW, Luo RX, Dei Santi A, Postigo AA, Dean DC. Cdk phosphorylation triggers sequential intramolecular interactions that progressively block RB functions as cells move through G_1. Cell 1999;98:859–69.

Downloaded from mct.aacrjournals.org on September 19, 2021. © 2010 American Association for Cancer Research.

Published OnlineFirst April 27, 2010; DOI: 10.1158/1535-7163.MCT-09-1163

9. Nevins JR. The Rb/E2F pathway and cancer. Hum Mol Genet 2001; 10:699–703.
10. Scambia G, Lovergine S, Masciullo V. RB family members as predictive and prognostic factors in human cancer. Oncogene 2006;25:5302–8.
11. Muller H, Bracken AP, Vernell R, et al. E2Fs regulate the expression of genes involved in differentiation, development, proliferation, and apoptosis. Genes Dev 2001;15:267–85.
12. Ishida S, Huang E, Zuzan H, et al. Role for E2F in control of both DNA replication and mitotic functions as revealed from DNA microarray analysis. Mol Cell Biol 2001;21:4684–99.
13. Ren B, Cam H, Takahashi Y, et al. E2F integrates cell cycle progression with DNA repair, replication, and G(2)/M checkpoints. Genes Dev 2002;16:245–56.
14. Polager S, Kalma Y, Berkovich E, Ginsberg D. E2Fs upregulated expression of genes involved in DNA replication, DNA repair and mitosis. Oncogene 2002;21:437–46.
15. Wells J, Graveel CR, Bartley SM, et al. The identification of E2F1-specific target genes. Proc Natl Acad Sci U S A 2002;99:3890–5.
16. Takahashi Y, Rayman JB, Dynlacht BD. Analysis of promoter binding by the E2F and pRB families *in vivo*: distinct E2F proteins mediate activation and repression. Genes Dev 2000;14:804–16.
17. Brasca MG, Albanese C, Alzani R, et al. Optimisation of 6,6-dimethyl pyrrolo[3,4-*c*]pyrazoles: identification of PHA-793887, a potent CDK inhibitor suitable for intravenous dosing. Bioorg Med Chem 2010;18: 1844–53.
18. http://www.tm4.org.
19. http://www.bioconductor.org.
20. Wu Z, Irizarry RA, Gentleman R, Martinez Murillo F, Spencer F. A model based background adjustment for oligonucleotide expression arrays. John Hopkins University, Department of Biostatistics Working papers; 2004, Paper1.
21. http://www.ncbi.nlm.nih.gov/geo.
22. Sanges R, Cordero F, Calogero RA. oneChannelGUI: a graphical interface to Bioconductor tools, designed for life scientists who are not familiar with R language. Bioinformatics 2007;23:3406–8.
23. Whittaker SR, Te Poele RH, Chan F, et al. The cyclin-dependent kinase inhibitor seliciclib (R-roscovitine; CYC202) decreases the expression of mitotic control genes and prevents entry into mitosis. Cell Cycle 2007;6:3114–31.
24. Berkofsky-Fessler W, Nguyen TQ, Delmar P, et al. Preclinical biomarkers for a cyclin-dependent kinase inhibitor translate to candidate pharmacodynamic biomarkers in phase I patients. Mol Cancer Ther 2009;8:2517–25.
25. ClinicalTrials.gov record number NCT00996255.
26. Senderowicz AM. Flavopiridol: the first cyclin-dependent kinase inhibitor in human clinical trials. Invest New Drugs 1999;17:313–20.
27. Meijer L, Bettayeb K, Galons H. (R)-roscovitine (CYC202, seliciclib). In: Smith PJ, Yue EW, editors. Inhibitors of cyclin-dependent kinases as anti-tumor agents. Boca Raton (FL): CRC Press; 2006, p. 87–225.
28. Misra RN, Xiao H, Kim KS, et al. *N*-(cycloalkylamino)acyl-2-aminothiazole inhibitors of cyclin-dependent kinase 2. *N*-[5[[[5-(1,1-dimethylethyl)-2-oxazolyl]methyl]thio]-2-thiazolyl]-4-piperidinecarboxamide (BMS-387032), a highly efficacious and selective antitumor agent. J Med Chem 2004;47:1719–28.
29. Toogood PL, Harvey PJ, Repine JT, et al. Discovery of a potent and selective inhibitor of cyclin-dependent kinase 4/6. J Med Chem 2005; 48:2388–406.
30. Chu XJ, DePinto W, Bartkovitz D, et al. Discovery of [4-amino-2-(1-methanesulfonylpiperidin-4-ylamino)pyrimidin-5-yl](2,3-difluoro-6-methoxyphenyl)methanone (R547), a potent and selective cyclin-dependent kinase inhibitor with significant *in vivo* antitumor activity. J Med Chem 2006;49:6549–60.
31. Parry D, Guzi T, Seghezzi W, et al. *In vitro* and *in vivo* characterization of SCH-727965, a novel potent cyclin dependent kinase inhibitor. AACR Conference, Los Angeles (CA). 2007, Poster 4371.
32. Wyatt PG, Woodhead AJ, Berdini V, et al. Identification of *N*-(4-piperidinyl)-4-(2,6-dichlorobenzoylamino)-1*H*-pyrazole-3-carboxamide (AT7519), a novel cyclin dependent kinase inhibitor using fragment-based X-ray crystallography and structure based drug design. J Med Chem 2008;51:4986–99.
33. Jones CD, Andrews DM, Barker AJ, et al. The discovery of AZD5597, a potent imidazole pyrimidine amide CDK inhibitor suitable for intravenous dosing. Bioorg Med Chem Lett 2008;18:6369–73.
34. Brasca MG, Amboldi N, Ballinari D, et al. Identification of *N*,1,4,4-tetramethyl-8-{[4-(4-methylpiperazin-1-yl)phenyl]amino}-4,5-dihydro-1*H*-pyrazolo[4,3-*h*]quinazoline-3-carboxamide (PHA-848125), a potent, orally available cyclin dependent kinase inhibitor. J Med Chem 2009;52:5152–63.
35. Tan AR, Yang X, Berman A, et al. Phase I trial of the cyclin-dependent kinase inhibitor flavopiridol in combination with docetaxel in patients with metastatic breast cancer. Clin Cancer Res 2004;10: 5038–47.
36. Haddad RI, Weinstein LJ, Wieczorek TJ, et al. A phase II clinical and pharmacodynamic study of E7070 in patients with metastatic, recurrent, or refractory squamous cell carcinoma of the head and neck: modulation of retinoblastoma protein phosphorylation by a novel chloroindolyl sulfonamide cell cycle inhibitor. Clin Cancer Res 2004;10:4680–7.
37. Hsieh WS, Soo R, Peh BK, et al. Pharmacodynamic effects of seliciclib, an orally administered cell cycle modulator in undifferentiated nasopharyngeal cancer. Clin Cancer Res 2009;15:1435–42.
38. Bild AH, Yao G, Chang JT, et al. Oncogenic pathway signature in human cancers as a guide to targeted therapies. Nature 2006;439: 353–7.
39. Whitfield ML, George LK, Grant GD, Perou CM. Common markers of proliferation. Nat Rev Cancer 2006;6:99–106.
40. Alzani R, Albanese C, Locatelli G, et al. Biological characterization of the dual CDK2/TRKA inhibitor PHA-848125 [abstract 294]. Eur J Cancer Suppl 2008;6:94.
41. Boss DS, Schwartz GK, Middleton MR, et al. Safety, tolerability, pharmacokinetics and pharmacodynamics of the oral cyclin-dependent kinase inhibitor AZD5438 when administered at intermittent and continuous dosing schedules in patients with advanced solid tumors. Ann Oncol 2010;21:884–94.
42. Squires MS, Lock V, Adam J, et al. Identification of a predicted biologically effective dose of AT7519, a cyclin-dependent kinase inhibitor, in a phase I study. AACR 100th Annual Meeting 2009, Denver (CO). 2009, Poster 3588.
43. Camidge DR, Pemberton M, Growcott J, et al. A phase I pharmacodynamic study of the effects of the cyclin-dependent kinase-inhibitor AZD5438 on cell cycle markers within the buccal mucosa, plucked scalp hairs and peripheral blood mononucleocytes of healthy male volunteers. Cancer Chemother Pharmacol 2007;60: 479–88.
44. Chen HZ, Tsai SY, Leone G. Emerging roles of E2Fs in cancer: an exit from cell cycle control. Nat Rev Cancer 2009;9:785–97.

Downloaded from mct.aacrjournals.org on September 19, 2021. © 2010 American Association for Cancer Research.

Published OnlineFirst April 27, 2010; DOI: 10.1158/1535-7163.MCT-09-1163

AACR American Association for Cancer Research

Molecular Cancer Therapeutics

Transcriptional Analysis of an E2F Gene Signature as a Biomarker of Activity of the Cyclin-Dependent Kinase Inhibitor PHA-793887 in Tumor and Skin Biopsies from a Phase I Clinical Study

Giuseppe Locatelli, Roberta Bosotti, Marina Ciomei, et al.

Mol Cancer Ther 2010;9:1265-1273. Published OnlineFirst April 27, 2010.

Updated version	Access the most recent version of this article at: doi:10.1158/1535-7163.MCT-09-1163
Supplementary Material	Access the most recent supplemental material at: http://mct.aacrjournals.org/content/suppl/2010/05/11/1535-7163.MCT-09-1163.DC1

Cited articles	This article cites 36 articles, 10 of which you can access for free at: http://mct.aacrjournals.org/content/9/5/1265.full#ref-list-1
Citing articles	This article has been cited by 1 HighWire-hosted articles. Access the articles at: http://mct.aacrjournals.org/content/9/5/1265.full#related-urls

E-mail alerts	Sign up to receive free email-alerts related to this article or journal.
Reprints and Subscriptions	To order reprints of this article or to subscribe to the journal, contact the AACR Publications Department at pubs@aacr.org.
Permissions	To request permission to re-use all or part of this article, use this link http://mct.aacrjournals.org/content/9/5/1265. Click on "Request Permissions" which will take you to the Copyright Clearance Center's (CCC) Rightslink site.

Downloaded from mct.aacrjournals.org on September 19, 2021. © 2010 American Association for Cancer Research.